PHYSICAL REVIEW MATERIALS **6**, L091403 (2022)

**Letter**

# Birefringence induced by antiferroelectric switching in transparent polycrystalline $PbZr_{0.95}Ti_{0.05}O_3$ film

Pranab Parimal Biswas,[1,2,*] Cosme Milesi-Brault,[1,2,3,4] Alfredo Blázquez Martínez,[1,2,3] Naveen Aruchamy,[1,3]
Longfei Song,[1,3] Veronika Kovacova,[2,3] Sebastjan Glinšek,[2,3] Torsten Granzow,[2,3]
Emmanuel Defay,[2,3] and Mael Guennou[1,2,*]

[1]*Department of Physics and Materials Science, University of Luxembourg, 41 rue du Brill, L-4422 Belvaux, Luxembourg*
[2]*Inter-institutional Research Group Uni.lu–LIST on Ferroic Materials, 41 rue du Brill, L-4422 Belvaux, Luxembourg*
[3]*Materials Research and Technology Department, Luxembourg Institute of Science and Technology, 41 rue du Brill, L-4422 Belvaux, Luxembourg*
[4]*Institute of Physics of the Czech Academy of Sciences, Na Slovance 1999/2, 182 21 Prague, Czech Republic*

(Received 24 June 2022; revised 3 August 2022; accepted 17 August 2022; published 20 September 2022)

The most characteristic functional property of antiferroelectric materials is the possibility to induce a phase transition from a nonpolar to a polar phase by an electric field. Here, we investigate the effect of this field-induced phase transition on the birefringence change of $PbZr_{0.95}Ti_{0.05}O_3$. We use a transparent polycrystalline $PbZr_{0.95}Ti_{0.05}O_3$ film grown on $PbTiO_3/HfO_2/SiO_2$ with interdigitated electrodes to directly investigate changes in birefringence in a simple transmission geometry. In spite of the polycrystalline nature of the film and its moderate thickness, the field-induced transition produces a sizable effect observable under a polarized microscope. The film in its polar phase is found to behave like a homogeneous birefringent medium. The time evolution of this field-induced birefringence provides information about irreversibilities in the antiferroelectric switching process and its slow dynamics. The change in birefringence has two main contributions: One that responds briskly and a slower one that rises and saturates over a period of as long as 30 min. Possible origins for this long saturation and relaxation times are discussed.

DOI: 10.1103/PhysRevMaterials.6.L091403

Antiferroelectric (AFE) materials are related to the family of vastly used piezoelectric and ferroelectric (FE) materials. The concept of antiferroelectricity was first postulated by Kittel in 1951 and then experimentally demonstrated in $PbZrO_3$ (PZO) by Shirane *et al.* [1,2]. AFE materials are often described as being composed of two sublattices of dipoles with opposite directions, leading to a zero macroscopic polarization [3]. A sufficiently large electric field above a critical value ($E_{\mathrm{AFE-FE}}$) can force a phase transition to a polar phase. This field-induced transition is the main defining feature of AFE; it gives rise to their characteristic double hysteresis loop. For the last decade, a large portion of research has been dedicated to exploring this remarkable nature of AFEs for their potential applications in capacitors, actuators, and cooling devices [4–9].

In its bulk room-temperature phase, the archetypal AFE PZO is orthorhombic *Pbam*. It undergoes a transition to a cubic $Pm\bar{3}m$ phase at 230 °C [3]. The structure of its field-induced polar phase has been under controversy. A number of phases have been proposed, yet a rhombohedral phase with space group *R3c* seems to be the most commonly accepted one [10–12]. Both the nonpolar orthorhombic phase and the polar rhombohedral phase of PZO are birefringent; more precisely, optically biaxial and uniaxial, respectively. It is therefore natural to expect a change in birefringence at the phase transition, both in the orientation of the optical axes and the magnitude of birefringence. As a matter of fact, birefringence measurements have proven to be very insightful in general in studies of ferroic transitions, including PZO [13]. Field-induced birefringence changes, i.e., electro-optic effects, have been extensively studied in oxide FE materials [14–17]. However, the birefringence change occurring along with antiferroelectric switching has barely been reported for oxide AFE materials. The development of transparent lead-based AFE and advancement in thin-film growth technologies provided electrical and optical characterization opportunities even in pure PZO [18]. The relative lack of studies on this subject with the exception of Refs. [18,19], prompted us to delve into the field-induced AFE-FE phase transition via the birefringence effect. Keeping the potential application in transparent optoelectronic devices in mind, we utilize a transparent $PbZr_{0.95}Ti_{0.05}O_3$ (PZT) film to study the birefringence change caused by the field-induced AFE-FE phase transition in transmission geometry. The composition with 5 % of Ti has been selected in order to reduce the critical field.

A polycrystalline PZT film of thickness 1 μm was deposited by chemical solution deposition method on a fused-silica ($SiO_2$) substrate, coated with 23 nm of ALD (Atomic Layer Deposition) deposited $HfO_2$ buffer layer. Before further processing, $HfO_2$ film was annealed at 700 °C and crystallized in the monoclinic phase [20]. To induce a preferred orientation, a seed layer of $PbTiO_3$ (PTO) was deposited on the substrate prior to PZT film deposition. The preparation of solutions for PZT and PTO followed a standard method

---

[*] Authors to whom correspondence should be addressed: pranab.biswas@uni.lu, mael.guennou@uni.lu

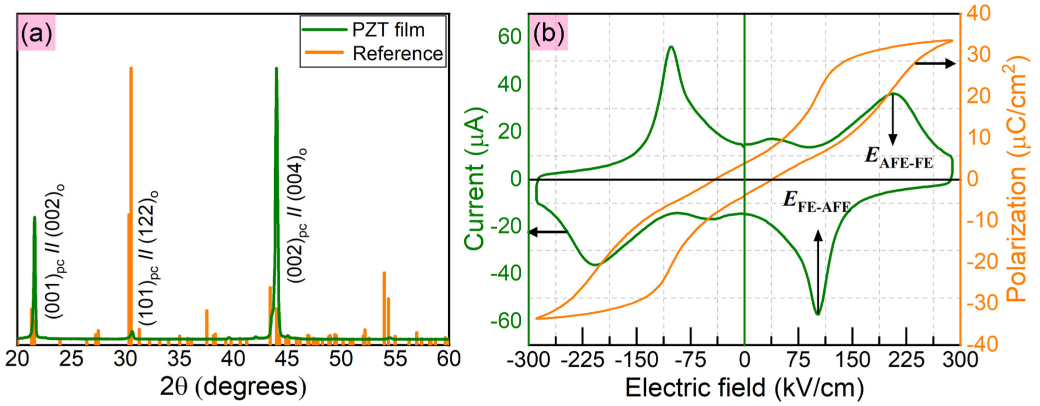

FIG. 1. (a) X-ray diffraction pattern of $PbZr_{0.95}Ti_{0.05}O_3$ film with reference peak intensities of $PbZrO_3$ (ICSD # 73469). (b) Polarization ($P$) versus electric field ($E$)/Current ($I$) versus electric field ($E$) loops measured at 100 Hz.

[21]. The film was fabricated by spin coating the PZT solution on the PTO seed layer. Every deposited layer was dried for 3 min at 130 °C and pyrolyzed for 3 min at 350 °C. After every four layers of depositions, the film was crystallized in a rapid thermal annealing furnace at 700 °C for 5 min in air. The process was repeated until the desired film thickness was reached. Platinum interdigitated electrodes (IDEs) with a gap of 10 $\mu$m and a finger width of 5 $\mu$m were patterned with lift-off photolithography.

X-ray diffraction (XRD) patterns of the PZT films (Bruker D8 Discover) are shown in Fig. 1(a). The pattern reveals that the film crystallizes in the perovskite phase, without any impurity phases, and with pronounced orientation along the $\langle 100\rangle$ pseudocubic direction. The $\langle 100\rangle$ pseudocubic direction could be associated with any of the two possible directions of the orthorhombic unit cell ($\langle 120\rangle_o$ and $\langle 002\rangle_o$). However, upon closer inspection and comparing the XRD pattern with the standard powder diffraction as shown in Fig. 1(a), we notice that the out-of-plane orientation of the film is specifically along the $\langle 002\rangle_o$ direction (subscripts "pc" and "o" refer to pseudocubic and orthorhombic indexing, respectively) [22]. To quantify the orientation of the film, a Lotgering factor was calculated using the intensity ratios of XRD peaks given in Ref. [23]. The Lotgering factor corresponding to $(00l)_{pc}$ orientation is approximately 0.86, indicating a strong preferred orientation. The in-plane orientation of the film, however, remains random.

The antiferroelectric hysteresis loop and the corresponding current curve were measured using a TF Analyzer 2000 from aixACCT by sending a bipolar triangular voltage ramp with a frequency of 100 Hz. The obtained result is shown in Fig. 1(b). The effective electric field across the IDE is derived from the applied voltage using the relation $E = V/(a + \Delta a)$ [24]. Here, $a$ is the gap between IDE fingers and $\Delta a = 1.324 t_f$, with $t_f$ being film thickness. From the switching loops, a broad $E_{\text{AFE}-\text{FE}}$ was noted with a maximum transition field of ~205 kV/cm, and the back transition to the nonpolar AFE phase ("back switching") occurs at 94 kV/cm ($E_{\text{FE}-\text{AFE}}$). As discussed in Ref. [25] the broad current peak results from the distribution of orientations in the plane of the film.

For the birefringence measurement, a polarizing optical microscope was used (Leica DM2700M). Figure 2(a) demonstrates a schematic of a general arrangement of the experimental setup used for field-induced birefringence measurements. The light intensity transmitted through the sample was recorded at a rate of 100 frames per second and analyzed using the image processing software ImageJ [26]. An area of 250 × 250 $\mu$m$^2$ was integrated in order to get an average total intensity.

For a birefringent single crystal, the intensity transmitted through crossed polarizers [27] is given by

$$\begin{aligned} I &= I_o \sin^2(2\varphi)\sin^2(\delta/2), \\ \delta &= (2\pi/\lambda)\,\Delta n * t, \end{aligned} \tag{1}$$

where $I_o$ is the incident light intensity, $\varphi$ the angle between the polarizer and the axes of the optical indicatrix of the crystal in the plane of the microscope stage, $\delta$ the phase retardation, $\lambda$ the wavelength of the light, $\Delta n$ the crystal's birefringence, and $t$ is the thickness of the crystal. When the polarization of the light passing through the crystal is parallel with either the polarizer's or the analyzer's axis, the crystal becomes dark. This is known as a position of extinction and is often used as a reference point. The maximum brightness is observed when the optical axis of the crystal is at an angle of 45° with respect to both polarizer and analyzer. For our polycrystalline film with random in-plane orientation, the total intensity collected is the sum of the intensities from individual grains. The grain orientations are random in the plane, but each grain is birefringent, so that a pristine film always transmits some light intensity. We therefore analyzed the transmitted intensity with the following formula:

$$I = I_{\text{Background}} + I_o \sin^2(2\varphi)\sin^2(\delta/2). \tag{2}$$

In addition to the parameters above, here, $I_{\text{Background}}$ is the intensity measured outside the electrode region, and the angle $\varphi$ is defined as the angle between the fingers of the IDE and the analyzer's axis [Fig. 2(a)]. We took 550 nm as the peak wavelength of our white light. $\Delta n$ becomes an effective birefringence that is a result of an orientational average.

Figure 2(b) displays images of PZT film under the polarizing microscope at $\varphi = 45°$, with and without field. A strong contrast between the electric field-OFF state and the electric field-ON state is visible to the naked eye. To confirm that the

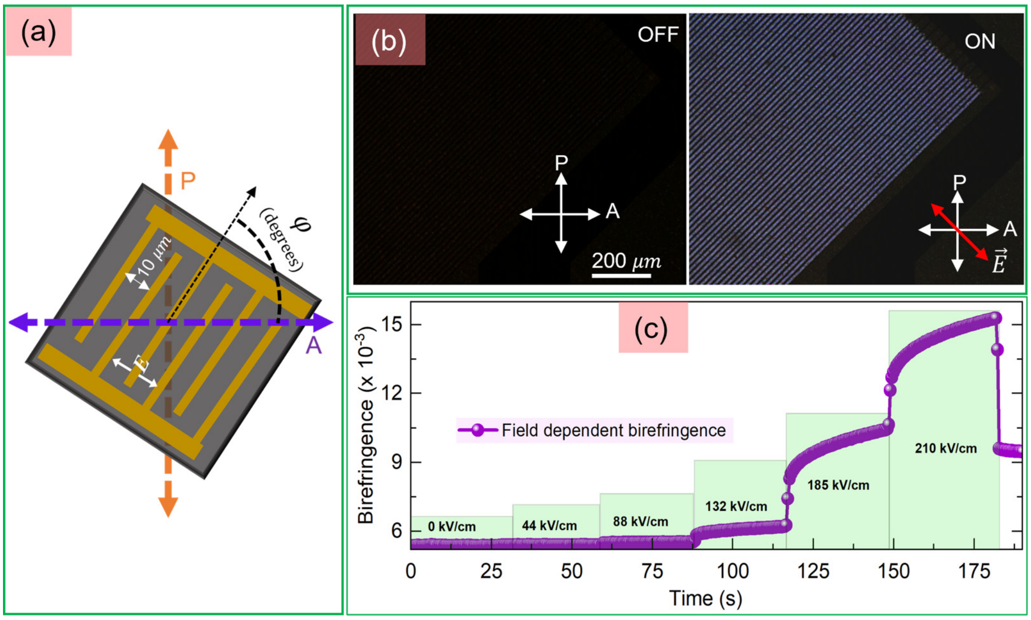

FIG. 2. (a) Schematic representation of birefringence measurement on PZT film under a polarizing microscope (top view). (b) Photographs of PZT film under the polarizing microscope in field-OFF and field-ON (205 kV/cm) states. (c) Electric-field dependence of birefringence. Here, A, P, and $E$ represent the light transmission axes of the analyzer, polarizer, and DC electric field, respectively.

observed birefringence is indeed linked to the phase transition, we performed this measurement with increasing values of the electric field. The results are displayed in Fig. 2(c). Small fields only caused a negligible response. The first prominent response is seen at 185 kV/cm, which is much closer to the $E_{\mathrm{AFE-FE}}$ phase transition field (205 kV/cm). The birefringence clearly increases with the field strength until 210 kV/cm. The field could not be increased beyond this value due to the electrical breakdown of the electrodes. The small response at the lower fields is probably because some of the crystallites start switching at lower fields as evident from the broad $E_{\mathrm{AFE-FE}}$ peak in the $I(E)$ loop shown in Fig. 1(b). However, the response is prominent only when the field is in the vicinity of or above the critical field. From the results discussed above, it is clear that the observed birefringence effect is indeed caused by the AFE-FE phase transition. The change in birefringence can therefore be seen as an effective electro-optic effect that sums up two main contributions: A change in intrinsic birefringence due to the change in crystal structure, but also a linear electro-optic effect that is forbidden in the AFE phase and becomes symmetry allowed in the polar phase.

In order to better analyze the birefringence caused by field-induced AFE-FE phase transition, we first measured the transmitted light intensity as a function of the angle $\varphi$ with and without field [Fig. 3(a)]. For a pristine sample, the light intensity is constant and independent of the sample orientation. This behavior can be easily related to the polycrystalline nature of the film. The PZT film is highly oriented along the $[001]_{\mathrm{pc}} \parallel [002]_{\mathrm{o}}$ direction but otherwise isotropic in plane. Orthorhombic PZO has principal refractive indices ($n_a < n_c < n_b$) along the directions of the crystallographic axes $a$, $b$, $c$ [28]. So, with light propagating along the $[002]_{\mathrm{o}}$ direction under a polarizing microscope, the relevant birefringence for a single grain is $(n_b - n_a)$ [29]. By averaging over all possible grain orientations in the plane of the film, one obtains an optically isotropic behavior whereby some light intensity is transmitted in a way that is independent of the angle $\varphi$.

When the electric field corresponding to the AFE-FE phase transition (205 kV/cm) is applied, the transmitted intensity follows a characteristic sine-squared-shape dependence that is consistent with Eq. (2) and the behavior of a homogeneous birefringent medium. This also is the result of an average over different possible orientations of crystallites in the observed area: If we assume that the field-induced polar phase has a rhombohedral structure and that all grains are switched into the polar phase, then their optical axis lies along the $[111]_{\mathrm{pc}} \parallel [042]_{\mathrm{o}}$ direction that is closest to the field direction, which results in a net transmitted intensity. Remarkably, after the field is switched off, the light intensity no longer behaves like a pristine sample but still shows a significant magnitude and $\varphi$ dependence. This points to an irreversible process upon the first application of the field. In Fig. 3(b), measurements are shown at two fixed positions ($\varphi = 0^\circ$ and $45^\circ$) as a function of time while switching the DC field ON and OFF in 10-s steps. For $\varphi = 45^\circ$ the intensity rises rapidly as soon as the field is turned on. The effect has a much smaller magnitude for the $\varphi = 0^\circ$ position. In these conditions, the change in birefringence appears reproducible from one step to another after the initial switching.

Figure 3(b) also shows that the birefringence during the field-ON duration is not constant over time but increases slowly for $\varphi = 45^\circ$, with a trend towards saturation. To better understand it, we carried out time-dependent birefringence measurements for various time intervals between field-ON and field-OFF states as exhibited in Fig. 4. We note three important observations in these measurements: (i) an increase

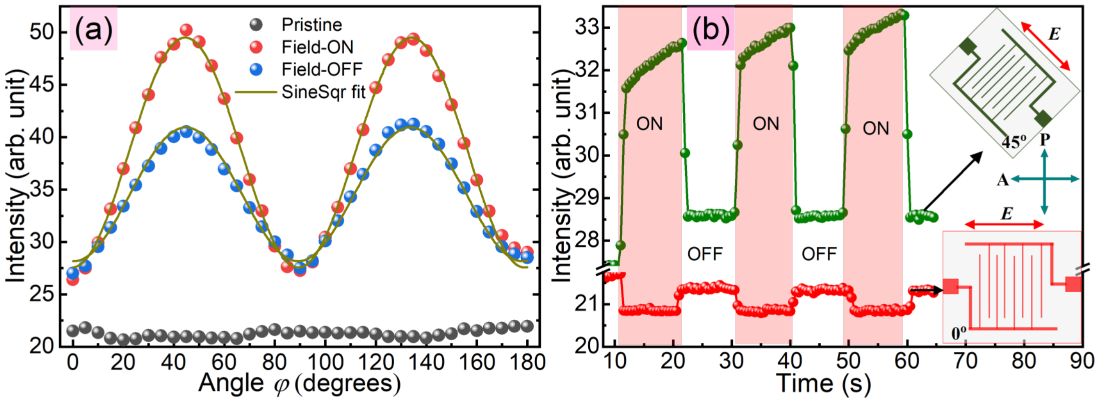

FIG. 3. (a) Azimuthal angular ($\varphi$) dependence of transmitted intensity for AFE phase (pristine), FE phase (field ON@205 kV/cm), and remnant (field OFF). (b) Field-induced (205 kV/cm) birefringence measurement at $\varphi = 0^\circ$ and at $\varphi = 45^\circ$. The time interval between each ON and OFF is 10 s. The inset shows schematics of the top view of the sample positions for $\varphi = 45^\circ$ and $\varphi = 0^\circ$.

in birefringence that occurs in two steps when the field is switched on, with a first swift jump followed by a much slower increase; (ii) the presence of a remnant birefringence i.e., an irreversible contribution that remains even after the field is switched off; and (iii) a significant undershoot upon back switching when the field is switched off, followed by a slow relaxation.

Switching of PZT-based antiferroelectric thin films under a DC electric field is reported to occur on a timescale of 6–10 ns, both forward (AFE-FE) and backward (FE-AFE) [30,31], i.e., it is instantaneous at the level of our measurement technique. The fast-responding component of the birefringence can therefore be associated with AFE-FE phase transition. The origin of the slow increase in birefringence could be linked to the growth and movement of newly formed domains and domain walls, respectively, in the polar phase under the DC electric field for a longer duration. This can be understood under the assumption that the polar phase is rhombohedral. The transition of the nonpolar orthorhombic to the polar rhombohedral phase comes with the formation of many domain walls (DWs) because of the absence of a group-subgroup relation. In the rhombohedral phase, we would have 180°, 71°, and 109° DWs. Under the applied field, the ferroelectric domains are expected to grow until saturation. This argument is verified from frequency-dependent $P(E)/I(E)$ hysteresis loop measurements where the saturation polarization ($P_s$) is

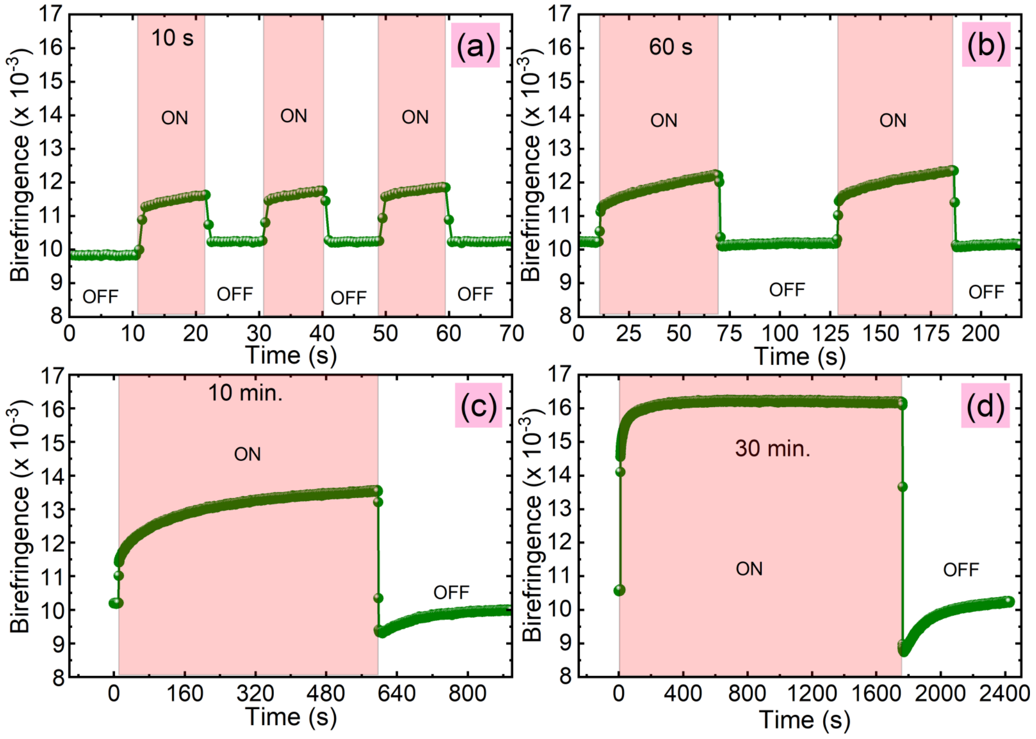

FIG. 4. Time-dependent birefringence measurement at $\varphi = 45^\circ$ for various intervals between field-ON (205 kV/cm) and field-OFF states: (a) 10 s, (b) 60 s, (c) 10 min, (d) 30 min.

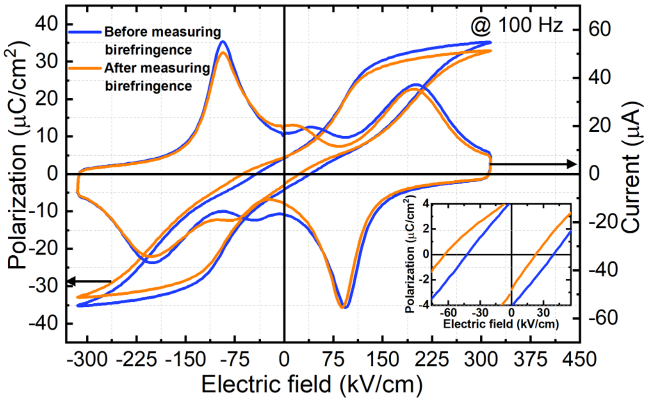

FIG. 5. $P(E)/I(E)$ hysteresis loops measured before (on a pristine film) and after the birefringent measurements. The inset shows a magnified view of the coercive field region.

seen to increase with a decrease in frequency (higher measurement time) without affecting the critical fields as displayed in Supplemental Material Fig. S1 [32]. The rate at which these DWs move could be affected by the presence of defects and dislocations through the pinning of DWs [33]. Moreover, with 71° and 109° DWs being ferroelastic in nature, the growth is accompanied by local stresses and strains causing a delay in the saturation.

The existence of a remnant birefringence points to an irreversible process, primarily, the irreversible FE domain formation due to the application of the high field. Figure 5 shows $P(E)/I(E)$ hysteresis loops measured before and after the birefringence measurements. The decrease in the saturation polarization and the critical fields point toward the FE domain stabilization. This is further validated by bipolar fatigue measurements shown in Fig. S2, where the effect is much more severe [32]. From the evolution of $P(E)/I(E)$ hysteresis loops during the electric fatigue measurement, it is noticed that the $P_s$ and critical fields decrease while the remnant polarization ($P_r$) increases with an increase in the number of cycles. The double hysteresis loop nearly becomes a single loop after $10^5$ cycles, suggesting the stabilization of the FE domains upon bipolar field cycling [34]. Another potential source of remnant birefringence is the small but finite polarization value observed at zero electric fields in the $P(E)$ hysteresis loop. The nonzero polarization in the present PZT film could originate either from the presence of intrinsic weak ferroelectricity in PZO-based antiferroelectric films or the additional polar PTO seed layer in spite of its small thickness (13 nm) compared to the PZT film [35,36]. The presence of the FE domain in AFE PZO is not unprecedented [37]. Besides, recent first-principle calculations suggest that the ground state of PZO is polar and ferrielectric rather the commonly accepted nonpolar antiferroelectric structure [38]. Thus, one cannot rule out the possibility that the finite remnant polarization observed at zero electric field in Fig. 1(b) is due to the presence of this ferrielectric phase.

Finally, the reason for the undershoot at the back switching and the slow relaxation that follows is not clear at this stage. Hypotheses can be made based on the presence of a space charge effect, mobile charged defects like oxygen vacancies or defect dipoles that are known to form during the high-temperature annealing of PZT film [39,40]. If we consider mobile charged defects, the application of a strong electric field for a long period could create a space charge effect, for example by migrating the charged defects near the grain boundaries, causing an internal bias field in the film. These defects could then redistribute themselves after the field is switched off. Similarly, if we consider polar defects, the application of a strong electric field for a long period could align defect dipoles with the field that then do not switch back when the field is switched off but provides a restoring force towards a stable state that is partially polarized. The relaxation time in both cases may vary from tens of minutes to days [41–43]. A thorough analysis of the observed relaxation is beyond the scope of this Letter, but we note that a similarly slow and isothermal transformation has been recently reported in a Nb-doped PZO crystal [44].

In summary, we studied the birefringence effect caused by field-induced AFE-FE phase transition in a transparent stack of antiferroelectric $PbZr_{0.95}Ti_{0.05}O_3/PbTiO_3/HfO_2/SiO_2$ thin film. We demonstrated that the observed birefringence is specifically induced by an AFE-FE phase transition. The azimuthal angle ($\varphi$) dependence of birefringence revealed that despite the polycrystalline nature, the PZT film in its field-induced polar phase behaves as a homogeneous birefringent medium. The time dependence of birefringence was probed for various intervals between field ON and field OFF. It was found that there are three components in the observed birefringence effect: (i) a fast-responding component associated with AFE-FE phase transition, (ii) a slow responding component due to ferroelectric and ferroelastic domains/domain walls growth/motion in the polar phase, and (iii) a remnant birefringence owing to the finite remnant polarization in the film and field-induced permanent FE domains. More generally, this work shows that this relatively simple protocol for birefringence measurements can be used as a sensitive probe for field-induced transitions in antiferroelectric thin films.

The data that supports the findings of this study are available from the corresponding authors upon reasonable request.

The authors would like to thank Uros Prah for his help in complementary measurements. This work is supported by the Luxembourgish National Research Fund (INTER/ANR/16/11562984/EXPAND and C16/MS/11348912/Guennou "BIAFET"). N.A. acknowledges financial support from Luxembourgish National Research Fund (FNR-PRIDE/15/10935404 "MASSENA"). A.B.M. and L.S. acknowledge financial support from the Luxembourgish National Research Fund under the project PACE (Photovoltaics: Advanced Concepts for high Efficiency, PRIDE/17/12246511/PACE). C.M.-B. was supported by the Operational Programme Research, Development, and Education (financed by European Structural and Investment Funds and by the Czech Ministry of Education, Youth, and Sports), Project No. SOLID21-CZ.02.1.01/0.0/0.0/16_019/0000760.

[1] C. Kittel, Theory of antiferroelectric crystals, Phys. Rev. **82**, 729 (1951).

[2] G. Shirane, E. Sawaguchi, and Y. Takagi, Dielectric properties of lead zirconate, Phys. Rev. **84**, 476 (1951).

[3] E. Sawaguchi, H. Maniwa, and S. Hoshino, Antiferroelectric structure of lead zirconate, Phys. Rev. **83**, 1078 (1951).

[4] S. Ke, M. Ye, P. Lin, H. Huang, B. Peng, Q. Sun, F. Wang, X. Peng, and X. Zeng, $PbZrO_3$-based antiferroelectric thin film capacitors with high energy storage density, Int. J. Adv. Appl. Phys. Res. **1**, 35 (2014).

[5] S.-T. Zhang, A. B. Kounga, W. Jo, C. Jamin, K. Seifert, T. Granzow, J. Rödel, and D. Damjanovic, High-strain lead-free antiferroelectric electrostrictors, Adv. Mater. **21**, 4716 (2009).

[6] X. Li, S.-G. (David) Lu, X. Chen, H. Gu, X. Qian, and Q. Zhang, Pyroelectric and electrocaloric materials, J. Mater. Chem. C **1**, 23 (2012).

[7] P. D. Thacher, Electrocaloric effects in some ferroelectric and antiferroelectric $Pb(Zr, Ti)O_3$ compounds, J. Appl. Phys. **39**, 1996 (1968).

[8] P. V. Castro, R. Faye, M. Vellvehi, Y. Nouchokgwe, X. Perpiñà, J. M. Caicedo, X. Jordà, K. Roleder, D. Kajewski, A. P.-Tomas, E. Defay, and G. Catalan, Origin of large negative electrocaloric effect in antiferroelectric $PbZrO_3$, Phys. Rev. B **103**, 054112 (2021).

[9] M. Valant, Electrocaloric materials for future solid-state refrigeration technologies, Prog. Mater. Sci. **57**, 980 (2012).

[10] B. Jaffe, W. R. Cook, and H. Jaffe, Properties of $PbTiO_3$, $PbZrO_3$, $PbSnO_3$, and $PbHfO_3$ plain and modified, *Piezoelectric Ceramics* (Academic, New York, 1971), pp. 115–134.

[11] S. E. Reyes-Lillo and K. M. Rabe, Antiferroelectricity and ferroelectricity in epitaxially strained $PbZrO_3$ from first principles, Phys. Rev. B **88**, 180102(R) (2013).

[12] J. Íñiguez, M. Stengel, S. Prosandeev, and L. Bellaiche, First-principles study of the multimode antiferroelectric transition in $PbZrO_3$, Phys. Rev. B **90**, 220103(R) (2014).

[13] I. Lazar, A. Majchrowski, A. Soszyński, and K. Roleder, Phase transitions and local polarity above $T_C$ in a $PbZr_{0.87}Ti_{0.13}O_3$ single crystal, Crystals **10**, 4 (2020).

[14] L. S. Kamzina and I. P. Raevskii, Electric field-induced birefringence in $Pb_{0.94}Ba_{0.06}Sc_{0.5}Nb_{0.5}O_3$ (PBSN-6) solid-solution single crystals, Phys. Solid State **47**, 1143 (2005).

[15] W. Jo, H. Cho, T. W. Noh, B. I. Kim, D. Kim, Z. G. Khim, and S. Kwun, Structural and electro-optic properties of pulsed laser deposited $Bi_4Ti_3O_{12}$ thin films on MgO, Appl. Phys. Lett. **63**, 2198 (1993).

[16] L. S. Kamzina, I. P. Raevskii, V. V. Eremkin, V. G. Smotrakov, and E. V. Sakhkar, Evolution of the optical properties of $Pb_{0.94}Ba_{0.06}Sc_{0.5}Nb_{0.5}O_3$ (PBSN-6) solid solution single crystals caused by a static electric field, Phys. Solid State **45**, 1112 (2003).

[17] S. Lee, T. W. Noh, and J. Lee, Control of epitaxial growth of pulsed laser deposited $LiNbO_3$ films and their electro-optic effects, Appl. Phys. Lett. **68**, 472 (1996).

[18] F. Wang, K. K. Li, and G. H. Haertling, Transverse electro-optic effect of antiferroelectric lead zirconate thin films, Opt. Lett. **17**, 1122 (1992).

[19] F. Wang, K. K. Li, E. Furman, and G. H. Haertling, Discrete electro-optic response in lead zirconate thin films from a field-induced phase transition, Opt. Lett. **18**, 1615 (1993).

[20] S. Glinšek, M. A. Mahjoub, M. Rupin,T. Schenk, N. Godard, S. Girod, J.-B. Chemin, R. Leturcq, N. Valle, S. Klein, C. Chappaz, and E. Defay, Fully transparent friction-modulation haptic device based on piezoelectric thin film, Adv. Funct. Mater. **30**, 2003539 (2020).

[21] N. Godard, P. Grysan, E. Defay, and S. Glinšek, Growth of {100}-oriented lead zirconate titanate thin films mediated by a safe solvent, J. Mater. Chem. C **9**, 281 (2021).

[22] H. Fujishita and S. Katano, Re-examination of the antiferroelectric structure of $PbZrO_3$, J. Phys. Soc. Jpn. **66**, 3484 (1997).

[23] F. K. Lotgering, Topotactical reactions with ferrimagnetic oxides having hexagonal crystal structures—I, J. Inorg. Nucl. Chem. **9**, 113 (1959).

[24] R. Nigon, T. M. Raeder, and P. Muralt, Characterization methodology for lead zirconate titanate thin films with interdigitated electrode structures, J. Appl. Phys. **121**, 204101 (2017).

[25] C. Milesi-Brault, N. Godard, S. Girod, Y. Fleming, B. El Adib, N. Valle, S. Glinšek, E. Defay, and M. Guennou, Critical field anisotropy in the antiferroelectric switching of $PbZrO_3$ films, Appl. Phys. Lett. **118**, 042901 (2021).

[26] W. S. Rasband, ImageJ. National Institutes of Health, Bethesda, Maryland, USA. http://imagej.nih.gov/ij (1997–2015).

[27] M. Born and E. Wolf, Optics of crystals, *Principles of Optics: Electromagnetic Theory of Propagation Interference and Diffraction of Light*, 7th ed. (Cambridge University Press, Cambridge, UK, 1999), p. 696.

[28] F. Jona, G. Shirane, and R. Pepinsky, Optical Study of $PbZrO_3$ and $NaNbO_3$ Single Crystals, Phys. Rev. **97**, 1584 (1955).

[29] S. Huband, A. M. Glazer, K. Roleder, A. Majchrowski, and P. A. Thomas, Crystallographic and optical study of $PbHfO_3$ crystals, J. Appl. Crystallogr. **50**, 378 (2017).

[30] T. K. Song, S. Aggarwal, Y. Gallais, B. Nagaraj, R. Ramesh, and J. T. Evans, Activation fields in ferroelectric thin film capacitors: Area dependence, Appl. Phys. Lett. **73**, 3366 (1998).

[31] S. S. N. Bharadwaja and S. B. Krupanidhi, Backward switching phenomenon from field forced ferroelectric to antiferroelectric phases in antiferroelectric $PbZrO_3$ thin films, J. Appl. Phys. **89**, 4541 (2001).

[32] See Supplemental Material at http://link.aps.org/supplemental/10.1103/PhysRevMaterials.6.L091403 for more discussion on frequency-dependent hysteresis loops and fatigue measurements on thin film.

[33] C. Yang, E. Sun, B. Yang, and W. Cao, Modeling dynamic rotation of defect dipoles and poling time dependence of piezoelectric effect in ferroelectrics, Appl. Phys. Lett. **114**, 102902 (2019).

[34] W. Geng, Y. Liu, X. Lou, F. Zhang, Q. Liu, B. Dkhil, M. Zhang, X. Ren, H. He, and A. Jiang, Polarization fatigue in antiferroelectric (Pb, La)(Zr, Ti)$O_3$ thin films: The role of the effective strength of driving waveform, Ceram. Int. **41**, S289 (2015).

[35] L. Pintilie, K. Boldyreva, M. Alexe, and D. Hesse, Capacitance tuning in antiferroelectric–ferroelectric $PbZrO_3-Pb(Zr_{0.8}Ti_{0.2})O_3$ epitaxial multilayers, New J. Phys. **10**, 013003 (2008).

[36] L. Pintilie, K. Boldyreva, M. Alexe, and D. Hesse, Coexistence of ferroelectricity and antiferroelectricity in epitaxial $PbZrO_3$ films with different orientations, J. Appl. Phys. **103**, 024101 (2008).

[37] X. Dai, J.-F. Li, and D. Viehland, Weak ferroelectricity in antiferroelectric lead zirconate, Phys. Rev. B **51**, 2651 (1995).

[38] H. Aramberri, C. Cazorla, M. Stengel, and J. Íñiguez, On the possibility that $PbZrO_3$ not be antiferroelectric, npj Comput. Mater. **7**, 196 (2021).

[39] N. Mukhin, D. Chigirev, L. Bakhchova, and A. Tumarkin, Microstructure and properties of PZT films with different PbO content—Ionic mechanism of built-in fields formation, Materials **12**, 2926 (2019).

[40] M. Dawber and J. F. Scott, A model for fatigue in ferroelectric perovskite thin films, Appl. Phys. Lett. **76**, 1060 (2000).

[41] P. Erhart, P. Träskelin, and K. Albe, Formation and switching of defect dipoles in acceptor-doped lead titanate: A kinetic model based on first-principles calculations, Phys. Rev. B **88**, 024107 (2013).

[42] B. Akkopru-Akgun, W. Zhu, M. T. Lanagan, and S. Trolier-McKinstry, The effect of imprint on remanent piezoelectric properties and ferroelectric aging of $PbZr_{0.52}Ti_{0.48}O_3$ thin films, J. Am. Ceram. Soc. **102**, 5328 (2019).

[43] C. Borderon, R. Renoud, M. Ragheb, and H. W. Gundel, Dielectric long time relaxation of domains walls in $PbZrTiO_3$ thin films, Appl. Phys. Lett. **104**, 072902 (2014).

[44] D. Kajewski, I. Jankowska-Sumara, J.-H. Ko, J. W. Lee, S. F. U. H. Naqvi, R. Sitko, A. Majchrowski, and K. Roleder, Long-term isothermal phase transformation in lead zirconate, Materials **15**, 4077 (2022).